DNA as a one-dimensional chiral material: Application to the structural transition between B form and Z form

Teruaki Okushima[1,*] and Hiroshi Kuratsuji[2]

[1]*Department of Physics, Ritsumeikan University, Kusatsu City, Shiga 525-8577, Japan*

[2]*Research Organization of Science and Engineering, Ritsumeikan University, Kusatsu City, Shiga 525-8577, Japan*

(Received 16 February 2011; revised manuscript received 10 June 2011; published 22 August 2011)

A dynamical model is presented for chiral change in DNA molecules. The model is an extension of the conventional elastic model, which incorporates the structure of base pairs and uses a spinor representation for the DNA configuration together with a gauge principle. Motivated by a recent experiment reporting chiral transitions between right-handed B-DNA and left-handed Z-DNA [Lee *et al.*, Proc. Natl. Acad. Sci. (USA) **107**, 4985 (2010)], we analyze the free energy for the particular case of linear DNA with an externally applied torque. The model shows that there exists, at low temperature, a rapid structural change depending on the torque exerted on the DNA, which causes switching in B and Z domain sizes. This can explain the frequent switches of DNA extension observed in experiments.

DOI: 10.1103/PhysRevE.84.021926 PACS number(s): 87.14.gk, 82.37.Rs, 87.15.A−

I. INTRODUCTION

Recent advances in experimental techniques have made it possible to perform experiments on the mechanical response of DNA molecules involving stretching and twisting of single DNA molecules [1,2]. It has been observed that external forces can bring about changes in the macroscopic conformation as well as the base-pair structure of DNA. For example, frequent structural changes have been observed between right-handed B-DNA and left-handed Z-DNA when minute negative torque is exerted on a DNA molecule [3]. In the regime of larger force, other structures, such as S-DNA, P-DNA, etc., are found [4], and the coexistence of these structures in stretch-twist diagrams has also been reported [5].

Along with the experimental studies, various theoretical attempts have been made to describe the mechanical responses of DNA. One typical theory known as the elastic rod model enables a description in terms of a simple mechanism of supercoiling and its effects [2,6–8]. Other significant theoretical models, such as the Poland-Scheraga model [9] and the Peyrard-Bishop-Dauxois model [10], are concerned with the problem of denaturation, and have been extended so as to include the coupling between DNA twisting and denaturation [11]. The interaction between DNA supercoiling and denaturation has been studied by extending the classical elastic rod model [12]. An effective potential model, which predicts twist-stretch coupling in the mechanical response of B-DNA, was presented in [13]. Statistical models that phenomenologically describe various structural transitions were developed in [14]. Several mesoscopic models have also been developed, which can describe the interaction between DNA conformation and *melting* structural transition [15,16]. However, there has not been a mechanical model of DNA that describes the interplay between the global configuration and the various intrinsic structures of DNA base-pairs, including B, Z, and S structures.

The purpose of this paper is to propose a phenomenological model that combines the aspects of conformation and intrinsic structure to obtain a clear picture of DNA mechanics. Our model adopts the Landau theory, which consists of the free energies for helical structures of base pairs connected by hydrogen bonds, elastic deformations of DNA configuration, and the interaction between them. The interaction is introduced by using the gauge principle with the spinor representation of DNA configuration. Monte Carlo simulation of the model is used to examine B-Z structural transitions of linear DNA under the application of external torques. It is found that there exists a cooperative effect, depending on both the temperature and the torque exerted on the DNA, which can be described in terms of the probability to create kink-antikink pairs. This cooperative effect causes sharp switching in B and Z domain sizes, which can explain the frequent switches of DNA extension observed in recent experiments [3].

II. MODEL

We use two kinds of order parameters: one is the order parameter for the conformations of DNA and the other is that for the intrinsic base-pair structures, which are determined by the hydrogen bonds between them. We first construct a moving frame that describes the conformation of the double-stranded DNA of N base pairs (bp's). Figure 1(a) shows a continuous parameter s representing the number of bases from one end of the molecule, where the DNA helical axis is parametrized as $\boldsymbol{r}(s)$. The normalized tangent vector along the axis is defined as $\boldsymbol{t} = \frac{1}{v}\frac{d\boldsymbol{r}}{ds}$, where v is the increase per bp along axis $\|d\boldsymbol{r}/ds\|$. A moving frame is defined at each point s by the set of three mutually orthogonal vectors $(\boldsymbol{b},\boldsymbol{n},\boldsymbol{t})$, where $\boldsymbol{b}$ is the normalized vector in the direction of base position and $\boldsymbol{n}$ is specified as $\boldsymbol{n} = \boldsymbol{t} \times \boldsymbol{b}$ to form a right-handed coordinate system.

We now introduce an order parameter to describe the configuration of the moving frame $(\boldsymbol{b},\boldsymbol{n},\boldsymbol{t})$, which is represented by a spinor Ψ: $\Psi = (\psi_1,\psi_2) \in \mathbb{C}^2$ with $|\psi_1|^2 + |\psi_2|^2 = 1$. The spinor is parametrized by a set of Euler angles, as in [17]. Using Euler angles (θ,ϕ,χ) as depicted in Fig. 1(b), the spinor is written as

$$\Psi = \left(\cos\frac{\theta}{2}e^{-i\frac{\phi+\chi}{2}}, \sin\frac{\theta}{2}e^{i\frac{\phi-\chi}{2}}\right)^t \tag{1}$$

*okushima@ike-dyn.ritsumei.ac.jp

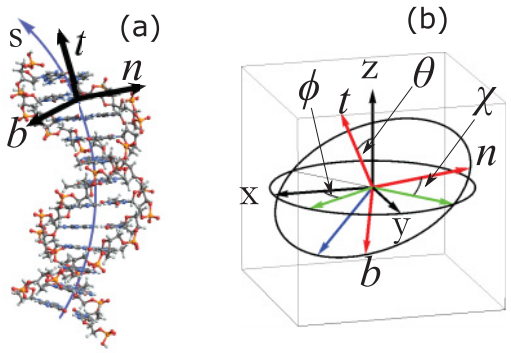

FIG. 1. (Color online) (a) The DNA molecule consists of two sugar-phosphate chains bridged by base pairs, forming the double helix. Moving frame vectors $(\boldsymbol{b},\boldsymbol{n},\boldsymbol{t})$ are defined along the helical axes parametrized by a continuous parameter s. (b) The frame vectors are specified by the depicted Euler angles (θ,ϕ,χ).

and $\boldsymbol{t}$ can be written as an average of the Pauli vector $\boldsymbol{\sigma}$ by the spinor: $\boldsymbol{t} = \Psi^\dagger \boldsymbol{\sigma} \Psi = (\sin\theta\cos\phi, \sin\theta\sin\phi, \cos\theta)$, where $\boldsymbol{\sigma}$ is given by $(\sigma^1,\sigma^2,\sigma^3)$ with the following Pauli matrices:

$$\sigma^1 = \begin{pmatrix} 0 & 1 \\ 1 & 0 \end{pmatrix}, \quad \sigma^2 = \begin{pmatrix} 0 & -i \\ i & 0 \end{pmatrix}, \quad \sigma^3 = \begin{pmatrix} 1 & 0 \\ 0 & -1 \end{pmatrix}.$$

We next consider an explicit form for the free energy of the DNA conformation, in terms of a functional of Ψ. To this end, we set the following requirements: (i) rotational symmetry and (ii) inclusion of up to first derivative with respect to s. Then, the simplest form satisfying these criteria is given by $F = \int_0^N \mathcal{F} ds$, where

$$\mathcal{F} = \mathcal{F}_s \equiv \frac{k_1}{2} \frac{d\Psi^\dagger}{ds} \frac{d\Psi}{ds} + \frac{k_2}{2} \left| \Psi^\dagger \frac{d\Psi}{ds} \right|^2. \tag{2}$$

With the use of the Euler angles, $\mathcal{F}_s$ reads $\frac{B}{2}[(\frac{d\theta}{ds})^2 + (\frac{d\phi}{ds})^2 \sin^2\theta] + \frac{C}{2}(\frac{d\phi}{ds}\cos\theta + \frac{d\chi}{ds})^2$, with $B = k_1/4$, $C = (k_1 + k_2)/4$, which is the well-known free-energy density of an elastic rod with isotropic bending elasticity B and torsional elasticity C [18]. Note here that, if an external force f in the z direction and torque τ are applied to the DNA ends, the free-energy density becomes $\mathcal{F}_s - f v \cos(\theta) - \tau L_k$, where L_k is the linking number of the DNA [6].

Now we introduce the order parameter ρ representing the internal structures of base pairs via gauge coupling with the conformational spinor. Consider the gauge transformation $\Psi \to \Psi \exp(i\alpha)$. If α is constant, the invariance of the free energy under the transformation is apparent, but if α has s dependence, the local gauge invariance does not hold. To keep the gauge invariance [19], we define the order parameter ρ for the internal structure of base pairs as a gauge field, which we call *chiral field*. ρ is the rotational angle between successive base pairs in the helix, $\rho > 0$ for right-handed rotation and $\rho < 0$ for left-handed rotation. After progressing ds, we have $\chi \to \chi + \rho ds$ and

$$\Psi^\parallel(s + ds) = \left(\psi_1 e^{-i\frac{\rho}{2}ds}, \psi_2 e^{-i\frac{\rho}{2}ds}\right)^t = \Psi - i\frac{\rho}{2}\Psi ds,$$

which just gives the parallel transport. Since the displacements of sugar-phosphate strings from the parallel transport $\Psi^\parallel(s)$ give rise to an elastic potential, we make the replacement of $d/ds \to D/Ds$ in Eq. (2), where D/Ds is the covariant derivative such that

$$\frac{D\Psi}{Ds} \equiv \lim_{ds\to 0} \frac{\Psi(s+ds) - \Psi^\parallel(s+ds)}{ds} = \frac{d\Psi}{ds} + i\frac{\rho}{2}\Psi.$$

The resulting free-energy density becomes $\mathcal{F}_s + \mathcal{F}_{s\rho}$, where $\mathcal{F}_{s\rho} = -iC\rho(\Psi^\dagger \frac{d\Psi}{ds} - \frac{d\Psi^\dagger}{ds}\Psi) + C\frac{\rho^2}{2}$; thereby, we have a new coupling term $\mathcal{F}_{s\rho}$ between the spinor field and the chiral field. In terms of the Euler angles, the coupling term is given by

$$\mathcal{F}_{s\rho} = -C\rho\left(\frac{d\chi}{ds} + \frac{d\phi}{ds}\cos\theta\right) + \frac{C\rho^2}{2},$$

from which we see that $C\rho$ is conjugate to the angular velocity with respect to s around $\boldsymbol{t}$ ($\Omega_3 \equiv \frac{d\chi}{ds} + \frac{d\phi}{ds}\cos\theta$). Combining the above two terms, the total free-energy density $\mathcal{F}_{s+\rho}$ can be written in terms of the Euler angles:

$$\mathcal{F}_{s+\rho} = \frac{B}{2}\left[\left(\frac{d\theta}{ds}\right)^2 + \left(\frac{d\phi}{ds}\right)^2 \sin^2\theta\right] + \frac{C}{2}\left(\frac{d\phi}{ds}\cos\theta + \frac{d\chi}{ds} - \rho\right)^2. \tag{3}$$

This is similar to the elastic rod model [6], but differs in the point that there is a coupling with the chiral field ρ. The conventional elastic rod model does not allow the inclusion of such a coupling term, because it does not take into account the deformation degrees of freedom coming from the base pairs, whereas in our case the spinor representation enables us to take into account such degrees of freedom naturally as a gauge field through the covariant derivative.

Now Landau's free energy for base-pair structures is defined by a general functional of the above-introduced chiral field $\rho(s)$ and the length scale $v(s) = \|d\boldsymbol{r}/ds\|$. The free-energy density $\mathcal{F}_b$ is given by

$$\mathcal{F}_b = \frac{d_1}{2}\left(\frac{d\rho}{ds}\right)^2 + \frac{d_2}{2}\left(\frac{dv}{ds}\right)^2 + \cdots + V(\rho, v, \ldots). \tag{4}$$

Here the last term is the effective potential, whose local minima, $(\rho_B, v_B, \ldots)$, $(\rho_Z, v_Z, \ldots)$, $(\rho_S, v_S, \ldots)$, etc., can be assigned to the locations of the base-pair structures B-DNA, Z-DNA, S-DNA, etc., respectively. On the other hand, the gradient terms represent additional free-energy costs due to changing base-pair structures along s.

In this way, we have constructed the total free-energy density for DNA as

$$\mathcal{F} = \mathcal{F}_{s+\rho} + \mathcal{F}_b. \tag{5}$$

It should be noted that the coefficients B, C can be extended to be functions of the order parameters for base-pair structure [20]. Our model contains the conventional elastic model as a limiting case of the rigid base-pair limit, $V(\rho) = -\delta(\rho - \omega_0)$. Namely, the latter is obtained by substituting ω_0 for ρ in Eq. (3). In the rigid sugar-phosphate limit $C \to \infty$, it recovers the model given in Ref. [21], becoming nonlocal in the sense that it contains the second derivative of the order parameter.

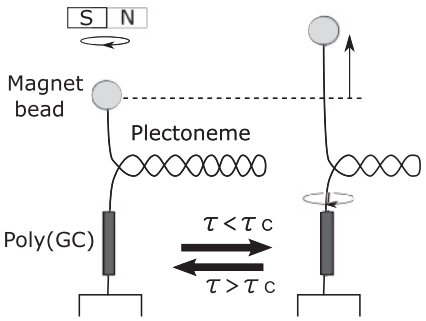

FIG. 2. Schematic representation of the experiment in Ref. [3] (see text).

III. CHIRAL TRANSITION INDUCED BY EXTERNAL TORQUE

As the first application of our model to realistic conditions, we consider the experiment performed by Lee *et al.* in Ref. [3]. In the experiment, shown schematically in Fig. 2, the ends of a DNA molecule were fixed with a glass cover slip and a magnetic bead, respectively. By applying negative torque to the DNA with the bead, minute negative superhelicity was induced in the DNA and then an interwinding DNA configuration, called *plectoneme*, was formed. Below the plectoneme, in the linear part of the DNA, there was a poly(GC) sequence that tends to change structures between B-DNA and Z-DNA. They measured frequent sharp changes of the DNA extension between the cover slip and the bead, as well as frequent B-Z transitions in the poly(GC) part. Therein, the B-Z transitions induce winding and unwinding of the plectonemic conformation, resulting in the observed sharp switches between small and large DNA extensions, respectively.

To analyze this experiment, it is sufficient to consider a model of a linear DNA molecule with B-Z structural transitions. By setting $\theta = 0, \phi = 0$ in Eq. (3), we obtain the total free-energy density given by

$$\mathcal{F} = \frac{C}{2}\left(\frac{d\chi}{ds} - \rho\right)^2 + \frac{d_1}{2}\left(\frac{d\rho}{ds}\right)^2 + V(\rho) - \tau\frac{d\chi}{ds}, \qquad (6)$$

where we adopt the following values: $C = 91 \times 10^{-20}$ J, $d_1 = D_1/\omega_0^2$ with $D_1 = 4.1 \times 10^{-21}$ J and $\omega_0 = 0.6$ rad/bp, and τ is the torque applied to the end of the linear DNA molecule. The potential density $V(\rho)$ is given by

$$V(\rho) = V_0[(\rho/\omega_0)^2 - 1]^2 + \tau_c\rho, \qquad (7)$$

with $\tau_c = -7.9 \times 10^{-21}$ J [22] and $V_0 = 6 \times 10^{-20}$ J, where the B-DNA and Z-DNA conformations correspond to the minima at around $\rho = \omega_0$ and $-\omega_0$, respectively. These parameter values are determined as follows. We expect the twist persistence length is 75 nm, which gives $C = 75$ nm $\times$ $k_BT_R/0.34$ nm $= 221k_BT_R = 91 \times 10^{-20}$ J, where T_R denotes room temperature and $k_BT_R = 1.38 \times 10^{-23}$ J K^{-1} $\times$ 300 K $= 4.1 \times 10^{-21}$ J is used. In our model, $\frac{d_1}{2}(d\rho/ds)^2$ gives the energy cost for structure change, which was already given in Ref. [21] by $2k_BT_R = 8.2 \times 10^{-21}$ J. From the equality $\frac{d_1}{2}(2\omega_0)^2 = 2k_BT_R$, one obtains $d_1 = D_1/\omega_0^2$, where $D_1 = k_BT_R = 4.1 \times 10^{-21}$ J. As to V_0, we adopt the value $V_0 = 6 \times 10^{-20}$ J ($\sim 15k_BT_R$) according to Ref. [21]. With this value, the domain-wall energy of our model ($E_{B-Z} = 8/3\sqrt{2d_1V_0\omega_0}$ [23]) agrees with the "B-Z junction energy" 5 Kcal/mol, which was estimated in Ref. [24]. The free energy of Z conformation is $E_Z = 2.3k_BT_R$ [14], thereby τ_c satisfies $2\omega_0\tau_c = -2.3k_BT_R$, which gives $\tau_c = -7.9 \times 10^{-21}$. Note that we have chosen the depths of minima that correspond to normal physiological conditions [25]. Furthermore, for simplicity, we have neglected the v dependency supposed in the general expression of Eq. (4).

To perform numerical simulation, we discretize the parameter s. The resulting free energy is given by

$$F = \sum_{i=1}^{N}\left[V(\rho_i) + \frac{C}{2}(\chi_i - \chi_{i-1} - \rho_i)^2 + \frac{d_1}{2}(\rho_i - \rho_{i-1})^2 - \tau(\chi_i - \chi_{i-1})\right], \qquad (8)$$

with $\chi_0 = 0$ and $\rho_0 = \omega_0$. By using the replica exchange Monte Carlo method [26], we sampled the equilibrium states, under various conditions of the external torque τ and temperature T. With every step, this method updates all replicas X_r with different temperatures T_r ($r = 1,2,\ldots$) simultaneously and then exchanges these replicas, to enhance the ergodicity of these samples. In the simultaneous updates, each replica $X_r = (\rho_1^{(r)}, \Delta\chi_1^{(r)}, \rho_2^{(r)}, \Delta\chi_2^{(r)}, \ldots, \rho_N^{(r)}, \Delta\chi_N^{(r)})$, where $\Delta\chi_i^{(r)} \equiv \chi_i^{(r)} - \chi_{i-1}^{(r)}$ (i.e., $\chi_i^{(r)} = \sum_{j=1}^{i}\Delta\chi_j^{(r)}$) follows the following steps:

(i) Draw a random integer i from 1 to N.

(ii) $\Delta\chi_i^{(r)}$ and $\rho_i^{(r)}$ are supposed to be shifted to $\tilde{\rho}_i^{(r)} = \rho_i^{(r)} + \epsilon_\rho R_{-1,1}$ and $\Delta\tilde{\chi}_i^{(r)} = \Delta\chi_i^{(r)} + \epsilon_\chi R_{-1,1}$, where ϵ_ρ and ϵ_χ are the values of maximum shifts for ρ and $\Delta\chi$, respectively, and $R_{-1,1}$ is a random number between -1 and 1.

(iii) Compute the free-energy change $\delta F = F(\tilde{X}_r) - F(X_r)$ and $W = \exp(-\beta_r\delta F)$, where $\beta_r = (k_BT_r)^{-1}$ with Boltzmann's constant k_B.

(iv) If $W > R_{0,1}$, then make changes $\Delta\chi_i^{(r)} = \Delta\tilde{\chi}_i^{(r)}$ and $\rho_i^{(r)} = \tilde{\rho}_i^{(r)}$; otherwise do not change.

After these simultaneous updates, for a randomly chosen neighboring pair of replicas, say X_r and X_{r+1}, exchange their configurations by the following acceptance criterion:

(i) Compute the cost function

$$\Delta = (\beta_{r+1} - \beta_r)[F(X_r) - F(X_{r+1})]$$

and $W = \exp(-\Delta)$.

(ii) If $W > R_{0,1}$, then exchange replicas as $(X_r, X_{r+1}) = (X_{r+1}, X_r)$; otherwise, do not exchange these replicas.

In the simulations, we set $\{\beta_r\} = \{0.01, 0.03, 0.05, 0.07, 0.1, 0.3, 0.5, 0.7, 1, 1.25, 1.5, 1.75, 2, 2.5, 3, 3.5, 4, 4.5, 5, 5.5, 6, 6.5, 7, 7.5, 8, 8.5, 9, 9.5, 10, 10.5, 11, 11.5, 12, 12.5, 13, 13.5, 14\}$, and confirmed the frequent exchanges of replicas. All the states are sampled at every $100N$ exchange Monte Carlo steps, after equilibration.

Figure 3(a) shows the average twists as functions of τ. We see that, at high temperatures compared to V_0, the response to τ is approximately uniform. In contrast, at relatively low temperatures, χ_N are susceptible to small differences in τ especially at around $\tau = \tau_c$. This result is in accord with the experiment of Ref. [3]. Namely, in the experiment, the torques

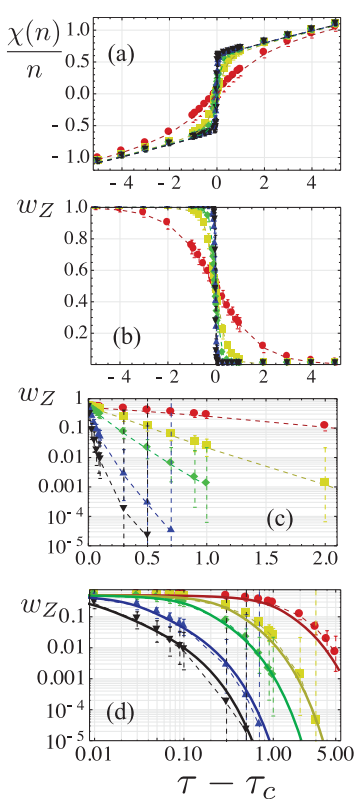

FIG. 3. (Color online) Exchange Monte Carlo results for $N = 100$ with 1000 samples: (a) χ_n/n ($n = 50$), (b) w_Z, (c) log plot of w_Z, (d) log-log plot of w_Z, as functions of $\tau - \tau_c$ for $\beta = 1$ (●, red), 3 (■, yellow), 5 (♦, green), 10 (▲, blue), and 14 (▼, black) in units of V_0 ($= 6 \times 10^{-20}$ J), where the vertical error bars on the data points represent their variances. w_Z is symmetric with respect to $(\tau, w_Z) = (\tau_c, 0.5)$. The ith bp is considered to be Z structure if $\rho_i < 0$. Solid lines in (d) are theoretical curves of Eq. (16) with fitted values $E_{B-Z} = 0.11V_0$ and $\gamma = 0.38$ [23]. Between $\chi(n)$ and w_Z, the approximate relation $d\chi/ds \simeq \rho_B + (\rho_Z - \rho_B)w_Z + \tau/C$ holds, where $\rho_B = 0.6$ and $\rho_Z = -0.6$.

applied to the linear part of DNA cannot be controlled to be a certain value but actually fluctuate around the value as

$$\delta\tau \sim \sqrt{Ck_BT/N} \sim 0.032V_0, \tag{9}$$

due to the disturbance from the rest of the DNA and/or the physiological buffer, and thus χ_N changes widely due to the high susceptibility to τ at around τ_c, since the experiment was carried out at low temperatures ($\beta V_0 \sim 14$). The large changes in χ_N alternate the winding number of the plectoneme, resulting in the change of DNA extension observed in the experiment.

We shall now confirm that the sensitivity of χ_N to τ is caused by the B-Z transition. For this, the Z-DNA ratio, w_Z, is plotted as functions of τ in Figs. 3(b)–3(d). This clearly shows that the sharp sensitivity of χ_N to τ at low temperatures found in Fig. 3(a) is coincident with the sharp decrease of w_Z, while the mild dependency of χ_N on τ at high temperatures is accompanied with a slow decrease of w_Z. Hence, our model clearly shows that the experimentally found sharp changes can be attributed to the dependency of B-Z transitions on torque, which becomes singular in the low-temperature limit.

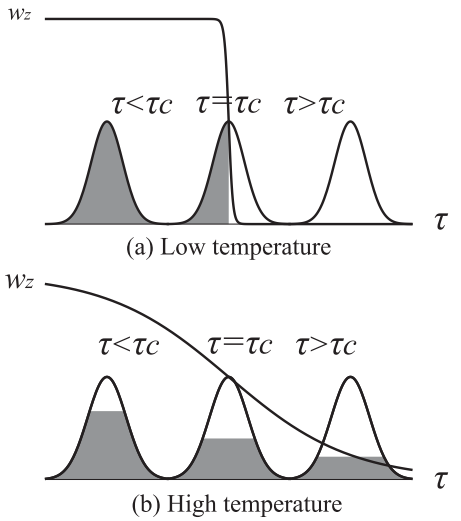

FIG. 4. Schematic illustration of torque responses of w_Z. (a) At low temperature, w_Z behaves like a switch. The three curves represent cases of torque distributions: the average τ satisfies $\tau < \tau_c$ (left), $\tau = \tau_c$ (middle), and $\tau > \tau_c$ (right). The fluctuations $\delta\tau$ are given by Eq. (9). Shaded regions in the distributions represent the ratios of Z-DNA conformations. (b) At high temperature, w_Z changes gradually as a function of τ, compared to $\delta\tau$. Hence, the ratios of Z conformations also change gradually, and do not show switching behaviors.

Let us discuss the details of the structural transition induced by external torque and the resulting singular responses, shown in Fig. 3. In low temperature such that $T/V_0 \sim 0$ (room temperature satisfies this condition), the response to torque is sharp, and then behaves like a switch. Hence, for example, if $\tau - \tau_c > 0$ is suddenly changed to $\tau - \tau_c < 0$, then all DNA structures nucleate from a false ground state (B-DNA) to a true ground state (Z-DNA). This point is illustrated in Fig. 4(a). Otherwise, if the superhelicity is set around "the midpoint value," then the torque fluctuates at around $\tau \sim \tau_c$, which induces the rapid structural switching observed in Fig. 5 A in Ref. [3]. Namely, we have confirmed that this switching induces the changes both in w_Z and in the change of DNA extension, dL. In contrast, when the temperature is high ($T/V_0 > 1$), the response becomes gradual, as shown in Fig. 4(b). In this case, we can neither expect the *switching* behavior in w_Z nor dL. In this way, with the use of our model, we have succeeded in clarifying the condition for stepwise change and for interconversion between these states observed in Ref. [3].

IV. NUCLEATION THEORY

Our findings can be explained in terms of the probability of kink-antikink nucleation and the average size of the metastable domain [27].

The variational equation $\delta F = 0$ reads

$$\frac{d\chi}{ds} - \rho - \frac{\tau}{C} = 0 \tag{10}$$

and

$$d_1 \frac{d^2\rho}{ds^2} = -\frac{dV_{\text{eff}}(\rho)}{d\rho}, \tag{11}$$

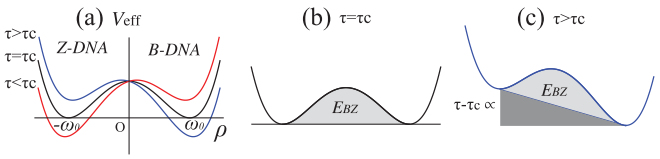

FIG. 5. (Color online) (a) Illustration for $V_{\rm eff}$ in Eq. (12) as functions of ρ: for $\tau < \tau_c$ (red), $\tau = \tau_c$ (black), and $\tau > \tau_c$ (blue). $V_{\rm eff}$ is symmetric at $\tau = \tau_c$. Parts (b) and (c) *schematically* show the domain-wall energy given by Eq. (15): (b) $E_{\rm B-Z}$ is the domain-wall energy for the symmetric $\tau = \tau_c$ case. In this case, the domain-wall energy corresponds to the shaded region. (c) For the $\tau \neq \tau_c$ case, the domain-wall energy requires the excess energy, shown in the darker shade of gray. This figure shows that the excess energy is proportional to $|\tau - \tau_c|$, as in Eq. (15).

where

$$V_{\rm eff}(\rho) = V_0\left[\left(\frac{\rho}{\omega_0}\right)^2 - 1\right]^2 - (\tau - \tau_c)\rho. \tag{12}$$

$V_{\rm eff}$ is depicted in Fig. 5(a) for various τ. For $\tau > \tau_c$, B conformation is stable while Z conformation is unstable. In contrast to this, for $\tau < \tau_c$, Z conformation is stable while B conformation is unstable. At $\tau = \tau_c$, $V_{\rm eff}$ is symmetric and these conformations are equally probable.

The probability P to form the nucleation is given by

$$P = [1 + e^{\beta E_{\rm nucl}(\tau)}]^{-1}, \tag{13}$$

where $E_{\rm nucl}(\tau)$ is the nucleation energy at torque τ. Since the nucleation starts with creating kink-antikink pairs, $E_{\rm nucl}$ is roughly estimated to be twice the domain-wall energy $E_{\rm dom}$ [28]:

$$E_{\rm nucl}(\tau) = 2E_{\rm dom}(\tau). \tag{14}$$

Then, the torque-dependence of the domain-wall energy is assumed to be

$$E_{\rm dom}(\tau) = E_{\rm B-Z} + \gamma|\tau - \tau_c|, \tag{15}$$

where $E_{\rm B-Z}$ is the domain-wall energy at $\tau = \tau_c$, shown in Fig. 5(b), and γ is the coefficient of torque in the domain-wall energy, shown in Fig. 5(c).

The distance between centers of neighboring metastable domains is estimated to be $1/P$. Once a metastable domain is created, it grows to a size r with the probability $\exp(-\beta\Delta V r)/\mathcal{N}$, where ΔV is the free-energy density difference and $\mathcal{N} = \int_0^{1/P} \exp(-\beta\Delta V r)dr$. The average domain size is estimated as

$$\begin{aligned}\langle r\rangle &= \int_0^{1/P} r e^{-\beta\Delta V r}/\mathcal{N} \\ &= P^{-1}\frac{1 + x - \exp x}{x(1 - \exp x)},\end{aligned}$$

with $x = \beta\Delta V/P$. From these results, the ratio of domain size between the metastable and the stable domain is given by $\langle r\rangle : P^{-1} - \langle r\rangle$. If $\tau > \tau_c$, then B-DNA is stable and Z-DNA is metastable and thus $w_{\rm Z} = \langle r\rangle P$. Otherwise, if $\tau < \tau_c$, then Z-DNA is stable and B-DNA is metastable and $w_{\rm Z} = 1 - \langle r\rangle P$. Putting these estimates together, we obtain

$$w_{\rm Z} = \frac{1 + x - e^x}{x(1 - e^x)}, \tag{16}$$

with

$$x = \beta(V_{\rm Z} - V_{\rm B})/P, \quad V_{\rm Z} - V_{\rm B} = 2\omega_0(\tau - \tau_c). \tag{17}$$

Let us confirm that Eq. (16) describes our numerical result of Fig. 3. The solid curves in Fig. 3(d) plot this relation (16), which agree with the numerical calculations.

We can also explain the singularity. Expanding $w_{\rm Z}$ around $\tau = \tau_c$ gives

$$w_{\rm Z} \simeq 0.5 - P^{-1}\beta\omega_0(\tau - \tau_c)/6, \tag{18}$$

where the slope with respect to τ is proportional to the average domain size $\sim P^{-1}$. Hence, the lower the temperature, the smaller the kink-antikink creation rate. Furthermore, the larger the average metastable size, the higher the structural susceptibility to torque. We therefore conclude that the temperature-dependent cooperative effect is the origin of the observed singularity.

This is analogous with the instability of a one-dimensional (1D) magnetic system. Actually, we see the clear correspondence with the 1D ferromagnetic Ising model:

$$\tau - \tau_c \leftrightarrow \text{magnetic field},$$

$$\text{domain-wall energy} \leftrightarrow \text{nearest-neighbor interaction}.$$

Hence, it is natural that the role of cooperativity (domain-wall energy divided by thermal energy) is essential to understand the results of Fig. 3. Furthermore, in the low-temperature limit, there occurs an instability at the external torque of $\tau = \tau_c$, which, in the Ising system, corresponds to zero external magnetic field [29].

Finally, we shall show that the twist dependence of transition rate reported in the experiment of Ref. [3] is qualitatively explained by this nucleation picture. Based on the above arguments on the nucleation energy (14), the nucleation energy from stable structure and from metastable structure are, respectively, given by

$$\begin{aligned}E_{\rm nucl} &= 2(E_{\rm B-Z} + \gamma|\tau - \tau_c|), \\ E^{\rm meta}_{\rm nucl} &= 2(E_{\rm B-Z} - \gamma|\tau - \tau_c|).\end{aligned}$$

Hence, the transition rates from B to Z structure and from Z to B structure, respectively, turn out to be, for $\tau > \tau_c$,

$$k_{\rm B-Z} = t_{\rm B}^{-1}e^{-\beta E_{\rm nucl}}, \quad k_{\rm Z-B} = t_{\rm Z}^{-1}e^{-\beta E^{\rm meta}_{\rm nucl}}, \tag{19}$$

and, for $\tau < \tau_c$,

$$k_{\rm B-Z} = t_{\rm B}^{-1}e^{-\beta E^{\rm meta}_{\rm nucl}}, \quad k_{\rm Z-B} = t_{\rm Z}^{-1}e^{-\beta E^{\rm meta}_{\rm nucl}}, \tag{20}$$

where $t_{\rm B}$,$t_{\rm Z}$ are the inverses of frequency factors for B and Z structures. From these results, the equilibrium constant $K_{\rm eq}$ ($\equiv k_{\rm B-Z}/k_{\rm Z-B}$) is given by $\frac{t_{\rm Z}}{t_{\rm B}}e^{-4\beta\gamma(\tau-\tau_c)}$. By noting that τ is related to superhelical density σ as $\tau = C\omega_0\sigma$ [30] and that B-Z transitions were observed at $\sigma = \sigma_c \sim -0.01$ in the experiment [3], we estimate that $C = \tau_c/\omega_0\sigma_c \sim 130 \times 10^{-20}$ J. Then, we obtain

$$K_{\rm eq} = \frac{t_{\rm Z}}{t_{\rm B}}e^{-4\beta\gamma C\omega_0(\sigma-\sigma_c)}, \tag{21}$$

where the coefficient of σ in the exponent is $4\beta\gamma C\omega_0 \sim 3 \times 10^2$. Here we used $T = 40\,^\circ$C and $\gamma = 0.37$ [fitted value in Fig. 3(d)]. Thus, the value of the coefficient of σ estimated here qualitatively agrees with, or, more properly speaking, is approximately one-fifth of the experimental value ($\sim 1.4 \times 10^3$) [31].

In summary, we have shown that our nucleation model not only provides a clear picture for the mechanically induced structural transition in DNA as the property of a one-dimensional chiral material, but also offers an explanation for recent experimental observations.

V. SUMMARY

We have constructed the single DNA mechanical model, which describes the interplay between intrinsic base-pair structures and global conformations. With this model, the mechanical responses of linear DNA to external torques were simulated and the singular response near $\tau = \tau_c$ was found in the low-temperature region. This singularity gives rise to instability of the B-Z transition with minute negative superhelicity, as in the experiment [3], which was explained in terms of the cooperative effect depending on the average size of the metastable domain. Furthermore, the twist dependency of the transition rate was qualitatively explained by the nucleation picture. These observations are analogous with the instability of a one-dimensional magnetic system: In the low-temperature limit, there occurs an instability at zero external magnetic field, which, in our system, corresponds to the external torque of $\tau = \tau_c$ [29]. From these estimates, we have a clear picture for the mechanically induced structural transition in DNA as one-dimensional chiral material.

We expect that this model will provide an additional basis for elucidating the structure-configuration interplay in higher-order biomolecular architectures, such as nucleosomes.

[1] T. Strick, J. Allemand, V. Croquette, and D. Bensimon, Prog. Biophys. Mol. Biol. **74**, 115 (2000).

[2] J. F. Marko, in *Multiple Aspects of DNA and RNA: From Biophysics to Bioinformatics*, Les Houches 2004, edited by D. Chatenay *et al.* (Elsevier, Amsterdam, 2005).

[3] M. Lee, S. H. Kim, and S.-C. Hong, Proc. Natl. Acad. Sci. (USA) **107**, 4985 (2010).

[4] C. Bustamante, Z. Bryant, and S. B. Smith, Nature (London) **421**, 423 (2003).

[5] Z. Bryant, M. D. Stone, J. Gore, S. B. Smith, N. R. Cozzarelli, and C. Bustamante, Nature (London) **424**, 338 (2003).

[6] J. F. Marko and E. D. Siggia, Science **265**, 506 (1994); J. F. Marko and E. D. Siggia, Phys. Rev. E **52**, 2912 (1995); C. Bouchiat and M. Mézard, Phys. Rev. Lett. **80**, 1556 (1998); B. Fain and J. Rudnick, Phys. Rev. E **60**, 7239 (1999).

[7] T. R. Strick, J. F. Allemand, D. Bensimon, A. Bensimon, and V. Croquette, Science **271**, 1835 (1996).

[8] B. C. Daniels, S. Forth, M. Y. Sheinin, M. D. Wang, and J. P. Sethna, Phys. Rev. E **80**, 040901(R) (2009).

[9] D. Poland and H. A. Scheraga, J. Chem. Phys. **45**, 1456 (1966).

[10] M. Peyrard and A. R. Bishop, Phys. Rev. Lett. **62**, 2755 (1989); T. Dauxois, M. Peyrard, and A. R. Bishop, Phys. Rev. E **47**, 684 (1993).

[11] S. Cocco and R. Monasson, Phys. Rev. Lett. **83**, 5178 (1999).

[12] T. B. Liverpool, S. A. Harris, and C. A. Laughton, Phys. Rev. Lett. **100**, 238103 (2008).

[13] R. D. Kamien, T. C. Lubensky, P. Nelson, and C. S. O'Hern, Europhys. Lett. **38**, 237 (1997); P. Nelson, Biophys. J. **74**, 2501 (1998); J. D. Moroz and P. Nelson, Macromolecules **31**, 6333 (1998).

[14] J. F. Léger, G. Romano, A. Sarkar, J. Robert, L. Bourdieu, D. Chatenay, and J. F. Marko, Phys. Rev. Lett. **83**, 1066 (1999); A. Sarkar, J. F. Léger, D. Chatenay, and J. F. Marko, Phys. Rev. E **63**, 051903 (2001).

[15] J. Yan and J. F. Marko, Phys. Rev. Lett. **93**, 108108 (2004).

[16] J. Palmeri, M. Manghi, and N. Destainville, Phys. Rev. Lett. **99**, 088103 (2007); M. Manghi, J. Palmeri, and N. Destainville, J. Phys. Condens. Matter **21**, 034104 (2009).

[17] See, e.g., J. J. Sakurai and J. J. Napolitano, *Modern Quantum Mechanics*, 2nd ed. (Addison-Wesley, Reading, MA, 2010).

[18] L. D. Landau, L. P. Pitaevskii, E. M. Lifshitz, and A. M. Kosevich, *Theory of Elasticity*, 3rd ed., Vol. 7 (Butterworth-Heinemann, Oxford 1986).

[19] A similar idea of a gauge principle has been previously used in the theory of liquid crystal: P. G. de Gennes and J. Prost, *The Physics of Liquid Crystals*, 2nd ed. (Oxford University Press, New York, 1993).

[20] If B,C depend on the structural order parameters, the gauge coupling and thus $\mathcal{F}_{s+\rho}$ become nonlinear and highly nontrivial.

[21] P. Jensen, Marko V. Jarić, and K. H. Bennemann, Phys. Lett. A **95**, 204 (1983).

[22] J. F. Marko, Phys. Rev. E **76**, 021926 (2007).

[23] See the discussion in Sec. IV and [28].

[24] L. J. Peck and J. C. Wang, Proc. Natl. Acad. Sci. (USA) **80**, 6206 (1983).

[25] The relative depths of minima depend on the salt concentration, as shown in Refs. [3,21].

[26] K. Hukushima and K. Nemoto, J. Phys. Soc. Jpn. **65**, 1604 (1996).

[27] The following discussion is similar to the nucleation theory in, e.g., J. S. Langer, Ann. Phys. (NY) **41**, 108 (1967).

[28] In the continuum limit, the kink (antikink) solution for the symmetric potential is given by $\rho(s) = \pm\omega_0 \tanh(\omega_0^{-1}\sqrt{2V_0/d_1}s)$. The corresponding domain-wall energy is estimated as $E_{\rm BZ} = \frac{8}{3}\sqrt{2d_1V_0}\omega_0 \simeq 0.6V_0$. This value is of the same order as the fitted value in Fig. 3.

[29] N. Goldenfeld, *Lectures on Phase Transitions and the Renormalization Group* (Perseus Books, Reading, Mass, 1992).

[30] The equation $\tau = C\rho\sigma$ is derived from $d\chi/ds = \rho + \tau/C, \sigma = (d\chi/ds - \rho)/\rho$, and $\rho \sim \omega_0$.

[31] The experimental value is obtained by finding the exponential curve fitting for the experiment of $K_{\rm eq}$ shown in Fig. 6(b) of Ref. 3. The experiment was done at a temperature of 40 °C.